Hydrogeologic Facies Characterization of an Alluvial Fan Near Fresno, California, Using Geophysical Techniques

By K.R. Burow, G.S. Weissmann, R.D. Miller, and G. Placzek

U.S. GEOLOGICAL SURVEY

Open-File Report 97-46

NATIONAL WATER QUALITY ASSESSMENT PROGRAM

6440-34

Sacramento, California
1997

U.S. DEPARTMENT OF THE INTERIOR
BRUCE BABBITT, Secretary

U.S. GEOLOGICAL SURVEY
Gordon P. Eaton, Director

For additional information write to:

District Chief
U.S. Geological Survey
Water Resources Division
Placer Hall
6000 J Street
Sacramento, CA 95819-6129

Copies of this report can be purchased from:

U.S. Geological Survey
Information Services
Box 25286
Federal Center
Denver, CO 80225

CONTENTS

FIGURES

TABLE

CONVERSION FACTORS, ABBREVIATIONS, AND ACRONYMS

Multiply	By	To Obtain
centimeter (cm)	0.3937	inch
kilometer (km)	0.6214	mile
meter (m)	3.281	foot
meter per second (m/s)	3.281	foot per second
square kilometer (km^2)	0.3861	square mile

Temperature is given in degrees Celsius (°C), which can be converted to degrees Fahrenheit (°F) by the following equation: $°F = 1.8(°C) + 32$.

Abbreviations and Acronyms

Hz, hertz (a unit of frequency of a periodic process equal to one cycle per second)
in., inch(es)
MHz, megahertz (a unit of measurement equal to one million hertz)
m/ns, meter(s) per nanosecond
µg/L, microgram(s) per liter
mg/L, milligram(s) per liter
ms, millisecond
ns, nanosecond

CDP, common-depth-point
DBCP, 1,2-dibromo-3-chloropropane
EM, electromagnetic
GPR, ground-penetrating radar
MCL, maximum contaminant level
TDS, total dissolved solids

Hydrogeologic Facies Characterization of an Alluvial Fan Near Fresno, California, Using Geophysical Techniques

by K.R. Burow, G.S. Weissmann, R.D. Miller, and G. Placzek

Abstract

DBCP (1,2-dibromo-3-chloropropane) contamination in the sole source aquifer near Fresno, California, has significantly affected drinking-water supplies. Borehole and surface geophysical data were integrated with borehole textural data to characterize the Kings River alluvial fan sediments and to provide a framework for computer modeling of pesticide transport in ground water. Primary hydrogeologic facies units, such as gravel, coarse sand or gravel, fine sand, and silt and clay, were identified in cores collected from three borings located on a 4.6-kilometer transect of multilevel monitoring wells. Borehole geophysical logs collected from seven wells and surface geophysical surveys were used to extrapolate hydrogeologic facies to depths of about 82 meters and to correlate the facies units with neighboring drilling sites. Thickness ranged from 0.3 to 13 meters for sand and gravel units, and from 0.3 to 17 meters for silt and clay. The lateral extent of distinct silt and clay layers was mapped using shallow seismic reflection and ground-penetrating radar techniques. About 3.6 kilometers of seismic reflection data were collected; at least three distinct fine-grained layers were mapped. The depth of investigation of the seismic survey ranged from 34 to 107 meters below land surface, and vertical resolution was about 3.5 meters. The ground-penetrating radar survey covered 3.6 kilometers and imaged a 1.5-meters thick, continuous fine-grained layer located at a depth of about 8 meters. Integrated results from the borehole sediment descriptions and geophysical surveys provided a detailed characterization over a larger areal extent than traditional hydrogeologic methods alone.

INTRODUCTION

A detailed characterization of the alluvial sediments along a 4.6-km transect was done to characterize the Kings River alluvial fan sediments and provide a framework for computer modeling of pesticide transport in ground water. Textural descriptions of continuous core were combined with borehole and surface geophysical data to characterize the vertical sequence and lateral extent of the interpreted hydrogeologic facies units. The results of this characterization contribute to a larger study of the environmental fate of DBCP (1,2-dibromo-3-chloropropane), an agricultural soil fumigant, in ground water in the eastern San Joaquin Valley, California.

Background

DBCP contamination in the sole-source aquifer near Fresno in the eastern San Joaquin Valley, California, has significantly affected drinking water supplies. DBCP persists in ground water at concentrations exceeding the maximum contaminant level (MCL) of 0.2 µg/L, although agricultural use of DBCP was banned in California in 1977. Understanding the processes that control the behavior of DBCP is critical in managing future ground-water resources.

One of the primary processes believed to affect DBCP concentrations is dispersion. Ground-water velocity may vary over several orders of magnitude due to heterogeneity of subsurface sedimentary textures. This variability in velocity leads to complex

spreading and mixing of solutes, such as DBCP. Numerical flow and transport modeling methods are being used to evaluate the effects of dispersion on DBCP concentrations in the aquifer; however, a detailed hydrogeologic characterization is needed to simulate dispersion using these numerical methods. This project is part of the U.S. Geological Survey's National Water Quality Assessment Program and is a cooperative effort of the University of California at Davis and the U.S. Geological Survey.

Purpose and Scope

The purpose of this paper is to present the methods and results of a detailed hydrogeologic characterization of a part of the alluvial aquifer and to demonstrate how the combined use of hydrogeologic and geophysical methods provides a more extensive characterization of the hydrogeologic setting than borehole core data alone. A combination of geologic coring and borehole and surface geophysical methods were used. Geophysical methods are a noninvasive, cost-effective means of extrapolating borehole hydrogeologic information. The borehole geophysical data were compared to core-derived lithologic descriptions and four textural categories were identified. These textural categories were further defined as distinct hydrogeologic facies that were then extrapolated using borehole and surface geophysical data.

Hydrogeologic facies, as described in this paper, refer to distinct lithologic units that were deposited by similar depositional processes and have similar hydraulic properties. Using conditional indicator (stochastic) methods, the field-scale data and interpretations were used to simulate the distribution of hydrogeologic facies over a large area while still preserving the smaller-scale features that are important to DBCP transport. Presentation of the stochastically generated hydrogeologic facies distributions is beyond the scope of this paper.

Description of Study Area

The study area is west of the foothills of the Sierra Nevada and east of the San Joaquin Valley trough on the high alluvial fan of the Kings River (fig. 1). The Kings River drains extensive watersheds of the central and southern Sierra Nevada. The Kings River alluvial fan, which encompasses about 2,500 km^2, contains sediments with significant vertical and lateral variability that were deposited as a result of the Pleistocene climate and associated glaciations (Cehrs and others, 1980). These fan deposits radiate from an apex near the city of Sanger. The recent migration of the Kings River to the south left remnant incised channels to the west of Sanger (Cehrs and others, 1980).

The principal aquifer in the study area is unconfined, and is contained mostly within the alluvial deposits of Pleistocene and Holocene ages (Page and LeBlanc, 1969). Water-bearing sand layers and gravel are locally confined by extensive clay layers, but the sands are interconnected at regional scale (Page and LeBlanc, 1969). Aquifer sediments consist of interbedded fine-grained and coarse-grained materials. The fine-grained deposits consist of predominantly sand, silt, and clay. The coarse-grained deposits consist of predominantly sand and gravel with occasional cobbles and boulders. Coarse-grained materials predominate near the head of the fan and the relatively fine-grained materials predominate at the toe (Page and LeBlanc, 1969). Regional movement of ground water is to the southwest. Locally, ground water is drawn toward Fresno because of heavy pumpage by local and municipal drinking water suppliers.

Previous authors have described the hydrogeologic facies present within the Kings River alluvial fan. Page and LeBlanc (1969) used drillers' logs to divide the alluvium laterally into facies on the basis of the ratio between coarse- and fine-grained materials, encompassing depths of 0 to 90 m. Cehrs and others (1980) presented results of extensive analysis of sedimentary facies as observed in core and logged in drillers' reports from wells located near Fresno; however, the sediments near Fresno are predominantly fine grained (containing less than 50 percent coarse-grained materials), and are derived from intermittent streams located north of the Kings River. In contrast, the sediments near the study site are derived from the Kings River, and the dominant facies contain more than 50 percent coarse-grained materials (plate 8 of Page and LeBlanc, 1969).

STUDY DESIGN AND METHODS

Continuous coring and borehole and surface geophysical methods were used to characterize the sediment textures and hydrogeologic facies (table 1). Twenty multilevel monitoring wells were drilled and installed at six sites along a 4.6-km transect between the spring of 1994 and summer of 1995 (fig. 2). Well depths at each drilling site ranged from 21 to 82 m. Although well installation along a transect may not be an ideal design for the purposes of characterization (presented in this paper), the transect was designed primarily to relate spatial and temporal changes in water quality to physical and chemical characteristics

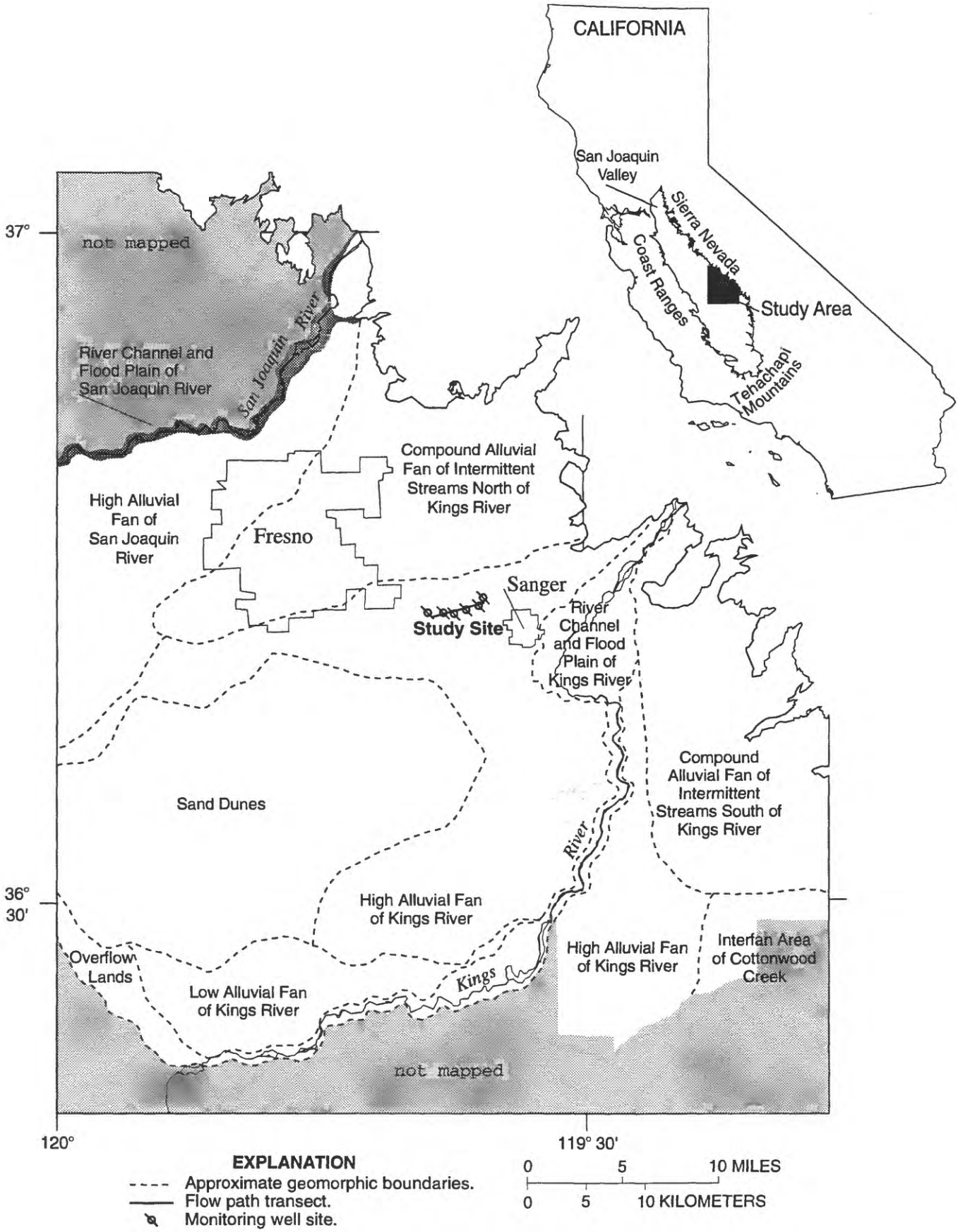

Figure 1. Location of geomorphic features of the study area (from Page and LeBlanc, 1969).

Table 1. Summary of hydrogeologic facies characterization data

[m, meter(s)]

Method	Type of data	Derived information
Borehole, continuous core	Direct observation of grain size, mineralogy, sorting Continuous in vertical line, descriptive, some measurements Depth of investigation 0 to 52.4 m	Provided basic textural categories, lithology Characterized vertical depositional sequences between units Textural unit thicknesses
Borehole, geophysical logs	In-situ measurement of electrical resistance adjacent to borehole Continuous in vertical line, quantitative Depth of investigation 0 to 80 m	Characterized vertical depositional sequences between units Textural unit thicknesses
Surface geophysics, seismic reflection	In-situ measurement of contrasts in acoustic properties of subsurface Continuous in vertical 2-D plane, quantitative Depth of investigation from 34 to 107 m	Continuity, lateral extent of fine-grained layers Location of units outside 2-D plane of well transect
Surface geophysics, ground-penetrating radar	In-situ measurement of contrasts in electrical properties of subsurface Continuous in vertical 2-D plane, quantitative Depth of investigation from 0 to 14 m	Continuity, lateral extent of fine-grained layers Location of units outside 2-D plane of well transect

of the aquifer. Thus, the wells are relatively closely spaced, and the transect is oriented approximately parallel to the direction of the ground-water gradient in the alluvial fan. About 3.6 km of seismic reflection and ground-penetrating radar (GPR) data were collected near the transect, with a depth of investigation ranging from 34 to 107 m for the seismic reflection, and 0 to 8 m for the GPR (table 1). A more detailed description of these methods is presented below.

Borehole Methods

Detailed sediment descriptions derived from continuous core were correlated with borehole geophysical logs to identify the textural categories from which the hydrogeologic facies were determined. By calibrating the borehole geophysical log responses to lithologic descriptions from the core, the lithology of intervals where core was not collected were estimated.

Two drilling methods were used to install the wells. Single, deep wells (about 80 m) were drilled and installed using a mud-rotary method at sites B1 and B3 (figs. 2 and 3). These wells were logged geophysically with an electromagnetic (EM) induction tool and a natural-gamma tool. The EM-induction tool measures the electrical conductivity of the materials surrounding the borehole. The probe used in this study is insensitive to the medium within about 7.5 cm of the borehole axis. Therefore, the effects of borehole fluid or formation disturbance are negligible in boreholes less than 15 cm in diameter (Williams, 1994). Total dissolved-solids (TDS) concentration in ground water, and the presence of silt and clay, affect the electrical conductivity of sediments measured by an induction logger. Because the TDS measured in these wells is relatively low (<500 mg/L), a high conductivity response is attributed to silt or clay lenses.

Several wells also were installed in single boreholes drilled using the mud-rotary drilling method at sites B2, B2.5, B3, and B4. Several geophysical logs—natural gamma, resistivity, and caliper—were collected in the mud-filled boreholes before the wells were finished. Natural gamma logs record the amount of gamma radiation emitted by geologic materials. The gamma-emitting radioisotopes that naturally occur in geologic materials are potassium-40 and products of the uranium and thorium decay series. Generally, clay-rich sediments emit relatively higher gamma radiation than do other sediments because of a relative abundance of potassium (decomposition of potassium feldspars) or uranium and thorium (adsorption and ion exchange) in fine-grained materials (Keys, 1990).

Resistivity logs are based on Ohm's law, which states that the rate of electrical current flow is directly proportional to the potential difference causing the flow, and inversely proportional to the resistance of the medium. The measured resistance of a medium depends on its composition, cross-sectional area, and path length (Keys, 1990). Several resistivity logs were collected, including lateral, short-normal, and long-normal resistivity. The open borehole diameter,

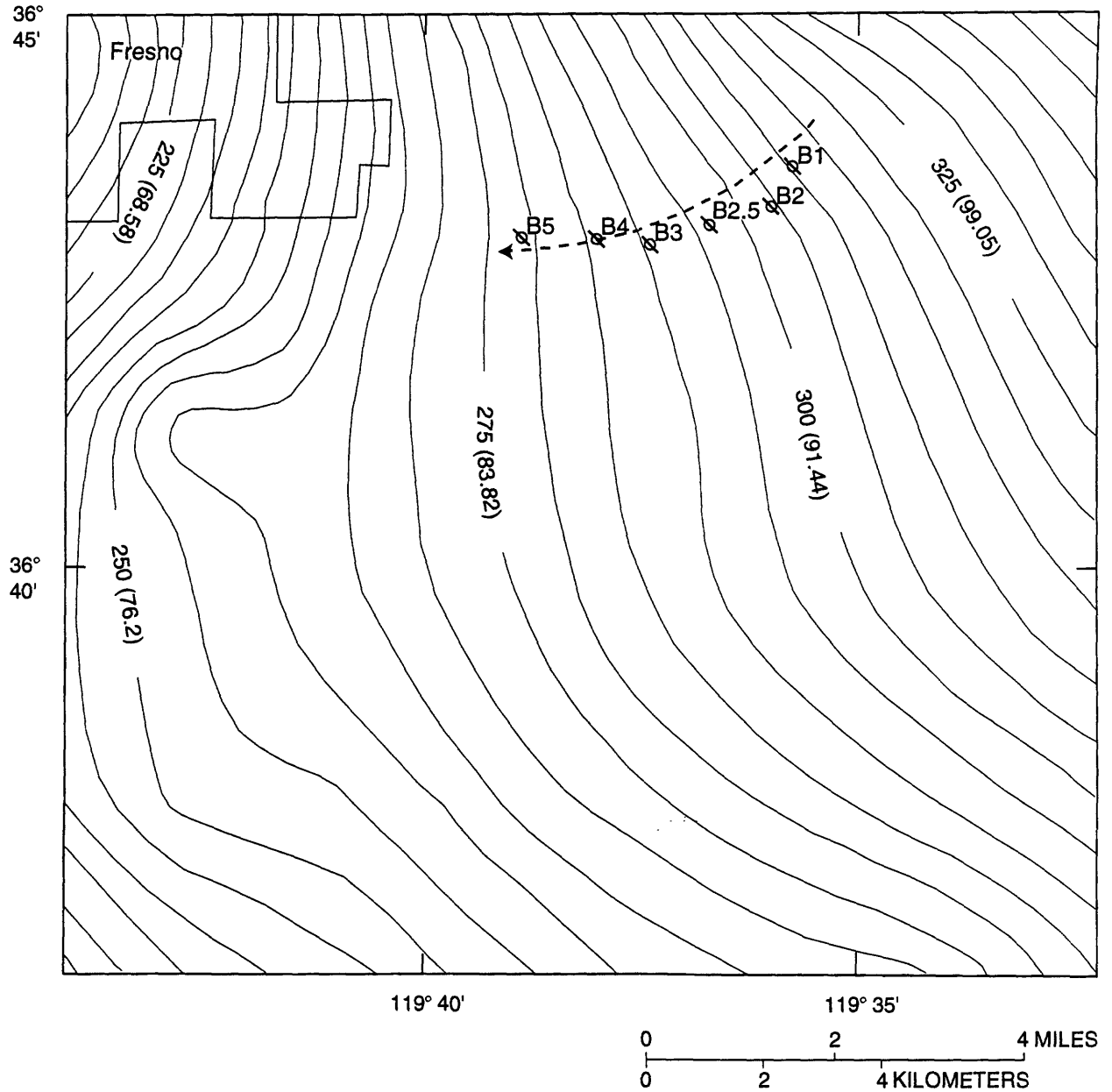

EXPLANATION

250 (76.2) — Line of equal ground water elevation, 1993, in feet (meters in parentheses).

B1 — Monitoring well drilling site.

Approximate regional ground-water flow direction.

Figure 2. Well transect drill sites. Wells are aligned nearly parallel to the regional ground-water gradient (from California Department of Water Resources, 1993).

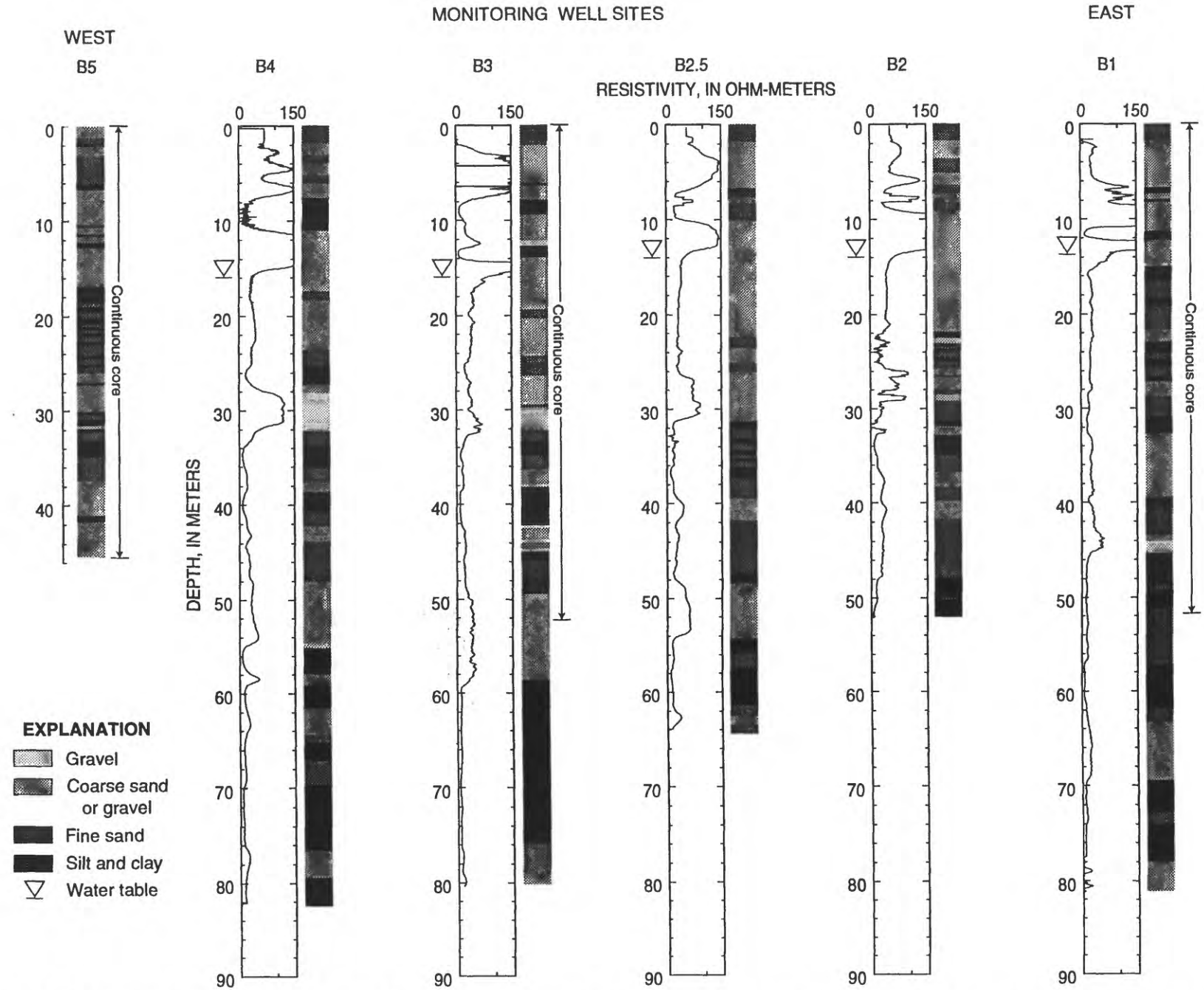

Figure 3. Hydrogeologic facies interpretations and accompanying borehole resistivity logs. Electromagnetic-induction logs were collected at drilling sites B1 and B3; lateral resistivity logs were collected at drilling sites B2, B2.5, and B4.

measured with a caliper tool, is important because some resistivity logs are particularly sensitive to changes in borehole diameter. Although all the logs were used to interpret the lithology at each site, only the lateral resistivity log is presented because these logs corresponded most closely to the EM-induction logs. The lateral resistivity log is an averaged resistivity value and, therefore, may not accurately represent lithology contacts.

Several wells were drilled and installed using a 6-5/8-in.-diameter hollow-stem auger. Continuous core was collected from three of the augered holes to depths of 52.1, 52.4, and 45.1 m at drilling sites B1, B3, and B5, respectively. A dry coring technique was used to avoid potential contamination during drilling. Core materials ranging from unconsolidated to semiconsolidated were collected using a wireline coring device with a split-barrel sampler lined with a 9-cm-diameter acrylic sleeve.

Surface Geophysical Methods

Surface geophysical methods can provide noninvasive, nearly continuous subsurface images. Two surface geophysical techniques—(1) shallow, high-resolution seismic reflection and (2) GPR—were used to map the location and lateral extent of fine-grained silt or clay layers. Characterization of the lateral continuity and extent of fine-grained layers is important in studying solute transport.

Shallow seismic reflection techniques have been used extensively in environmental studies to map features, such as depth to bedrock (Hunter and others, 1984; Miller and others, 1989), stratigraphic boundaries (Genau and others, 1994; Pullan and Hunter, 1991), and hydrologic boundaries (Birkelo and others, 1987). Continuous, high-resolution surface-geophysical profiles can provide a cost-effective, noninvasive alternative to traditional drilling methods (Haeni, 1986).

The seismic reflection method uses an artificial source to generate seismic (for example, acoustic) waves at land surface. The seismic energy travels vertically downward through the medium and is reflected at points where there is sufficient contrast in bulk density and seismic velocity— referred to as acoustic impedance—to generate a reflected wave that is detectable in geophones planted at the surface (Telford and others, 1990). In this study, the largest impedance contrasts, recorded as the highest-amplitude reflections, probably occur at transitions between coarse-grained, low seismic-velocity sediments (such as sands and gravel), and fine-grained, higher velocity sediments (such as silt and clay).

About 3.6 km of shallow, high-resolution seismic reflection data were collected in June 1994 near the well transect (fig. 4). Before data collection, a series of tests was done to optimize data quality at this study site. During these tests, the seismic source, geophone spacing and frequency, source-to-nearest-receiver offset, and recording parameters (such as analog filters and sampling frequency) were determined.

The seismic data were collected using a 24-fold common-depth-point (CDP) method (Dobrin, 1976) with end-on field geometry. The source-to-nearest receiver offset was 30 m, shot-spacing interval was 2.4 m, and single, 100-Hz (hertz) geophones were used at 1.2-m spacing. Data were filtered using an analog band-pass filter of 70 to 500 Hz, and recorded using an ES-2401X 48-channel seismograph with a sampling interval of 0.5 ms. Three vertical profiles, designated as lines 1, 2, and 3 (fig. 4), were completed in the vicinity of drilling site B3 using an auger-mounted 12-gauge buffalo gun acoustic source. Two more profiles, designated as lines 4 and 5, were completed near drilling site B2 using a 30.06 rifle acoustic source.

GPR is another surface geophysical method used in this study to map fine-grained layer continuity. Although the GPR mapped a relatively shallow zone above the water table, the stochastic simulations rely on information (such as vertical sequence and lateral continuity of hydrogeologic facies) from the entire sediment thickness. During July 1994, a GPR survey was made to complement the data obtained from the seismic survey. The GPR lines coincide with the seismic reflection survey lines and thus, have the same line number designation (fig. 4).

GPR has been used in hydrogeologic investigations to map depth-to-bedrock (Lieblich and others, 1992), depth-to-water, and depositional structure in alluvial settings (Wright and others, 1984; Beres and Haeni, 1991; Knoll and others, 1991; Barr, 1993). Similar to seismic reflection methods, the GPR method produces a virtually continuous cross-sectional image of contrasts in subsurface physical properties. However, rather than generating acoustic waves, GPR uses a series of EM pulses generated at the surface by a radio frequency transmitter antenna. The EM wave source has a much higher frequency than the seismic energy source, and the depth of penetration for the GPR survey is significantly less. The energy is reflected at boundaries of contrasting electrical properties of the subsurface sediments. Electrical properties are determined primarily by water content, dissolved minerals, expansive clay, and heavy-mineral content (Beres and Haeni, 1991). A portion of the energy is reflected back to the surface to a receiving antenna where wave energy is recorded as a function of time.

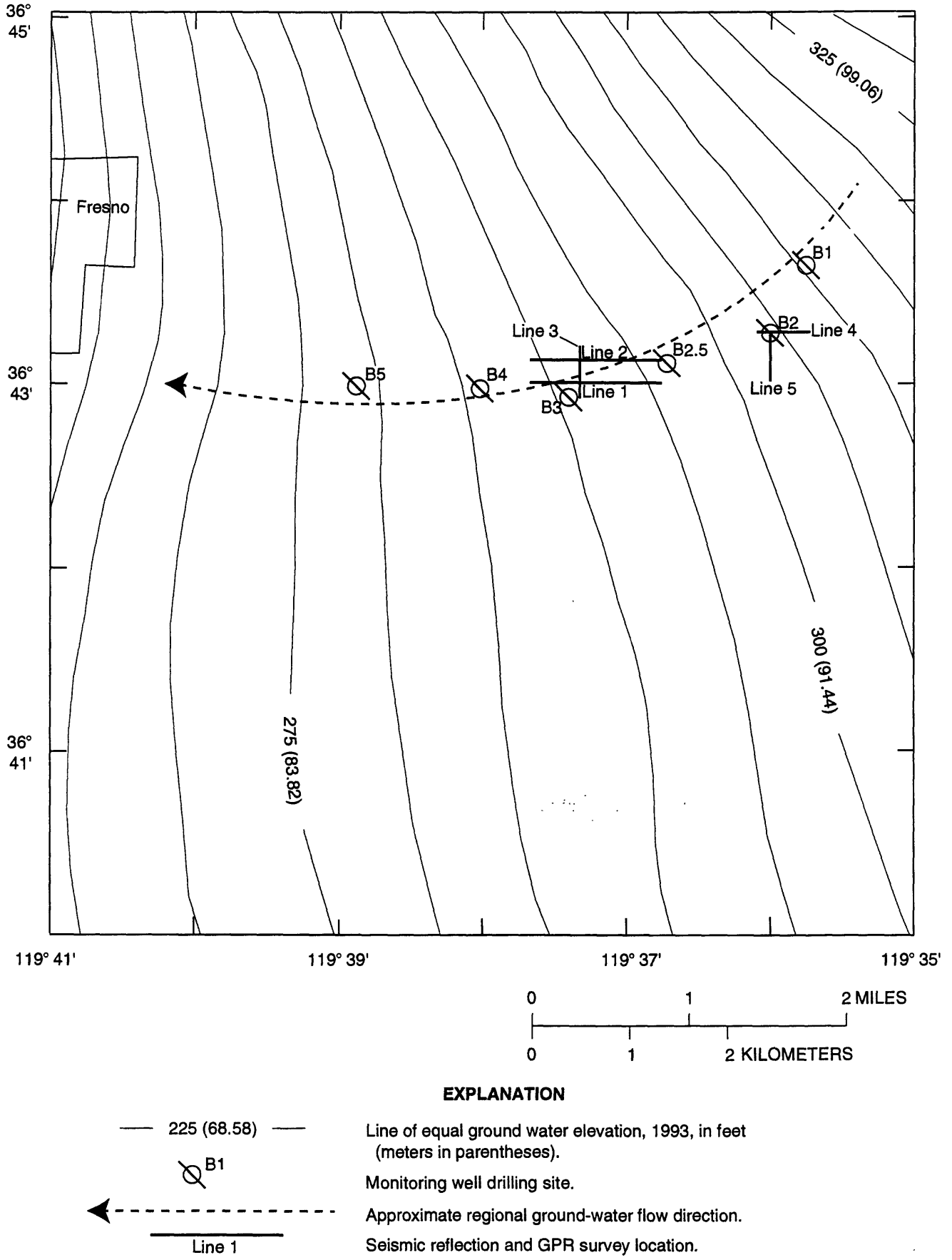

Figure 4. Location of seismic reflection and ground-penetrating radar (GPR) profiles.

Depth-to-reflectors can be calculated by inferring an average EM wave velocity and multiplying it by the one-way travel time to the reflector. In this study, two 100-MHz (megahertz) shielded, center-frequency antennas were used; a schematic representation of the GPR system is shown in Beres and Haeni (1991).

RELATION BETWEEN BOREHOLE TEXTURE AND GEOPHYSICS

Textural Descriptions

The sedimentary textures observed in the core are predominantly fine to medium sand, interlayered with poorly consolidated mudstone/siltstone, coarse sand, and gravel. These sediments are typical of the fluvial-dominated alluvial fan setting in which they were deposited. Four textural categories have been distinguished in the cores. The categories, in decreasing order of hydraulic transmissive properties, are gravel, coarse sand or gravel, fine sand, and silt and clay. The occurrence (in percent) of each category was calculated using the total footage of the core and the borehole geophysical logs (508 m). These textural categories were interpreted as hydrogeologic facies. In this study, hydrogeologic facies refer to distinct units that were deposited by similar sedimentary processes and are interpreted to have similar hydraulic properties.

The "gravel" category occurs in only 3 percent of the borings and consists of cobbles and gravel in a coarse to very coarse sand matrix. Cobbles range in size from 3 to 6 cm in diameter and are commonly metamorphic clasts. Grains are subrounded to rounded, poorly to moderately sorted, and have very little, if any, interstitial clay. These sediments probably represent channel lag deposits of paleo-Kings River channels.

The "coarse sand or gravel" category occurs in 46 percent of the borings and consists of massive, very coarse to medium sand, subrounded to rounded, and moderately to well sorted, and may contain some gravel. Some zones contain minor interstitial clay. Constituent grains are predominantly quartz with lesser amounts of biotite, muscovite, feldspar, and other mafic minerals. These sands may be primarily associated with channel bar deposits of the Kings River or other secondary streams. The thickness of the sand and gravel units ranges from 0.3 to 13 m.

The "fine sand" category is found in about 26 percent of the borings. Sediments in this category are laminated to massive, very fine to fine sand with subrounded to rounded grains that are moderately-to-well sorted. These sediments may be associated with secondary channels, crevasse splays, or proximal overbank deposits. Very fine to medium sands with interstitial clay and silt also are included in this category; these deposits may represent paleosol horizons.

The least transmissive category is "silt and clay," which consists of laminated to blocky silts and clay that contain some root casts. This category makes up 25 percent of the borings, and ranges in thickness from 0.3 to 17 m. Extensive silts and clays in this category were probably deposited as floodplain sediments.

Borehole Geophysics Integrated with Textural Descriptions

The sequence of hydrogeologic facies, categorized from the core descriptions from boreholes at drilling sites B1 and B3, was extrapolated below the cored depth using borehole geophysical logs. The geophysical logs also were used to correlate facies with neighboring boreholes. Selected geophysical logs for each drilling site are shown in cross section along with the log of interpreted facies categories for each borehole (fig. 3). Resistivity from EM-induction logs are shown for drilling sites B1 and B3, and lateral resistivity logs are shown for drilling sites B2, B2.5, and B4. No geophysical logs were collected at drilling site B5. Both geophysical tools provide relative measurements of resistivity near the borehole, although the magnitude of the resistivity value may differ between the two methods.

Although fewer textural data are available for the oldest sediments at the bottom of the section, it appears that there are significantly thick sequences of fine-grained material below about 60 m throughout the cross section (fig. 3). In general, the geophysical logs are not highly correlated with the sedimentary textural categories defined from the core. Some of the detail in the core is not apparent in the geophysical logs. However, the geophysical logs do show an increase in fine-grained textures below a depth of about 60 m. Drilling sites B1 and B3 appear to have somewhat different sequences of deposits below 60 m, suggesting that the orientation of the well transect may not be aligned exactly with individual depositional features.

A sequence of coarse sand lies above the deepest fine-grained deposits. These sands are generally more than 6 m thick and may be associated with the paleo-Kings River channel bar deposits. Coarse sands appear in all of the boreholes at similar depths; however, the degree of direct interconnection between boreholes may be limited because the channel meanders in and out of the cross section.

Following deposition of the coarse channel sands are alternating deposits of silt or clay and coarse sands. The coarsest materials in the entire section are found in an interval of coarse sand and gravel located in the range of 26 to 32 m below land surface. These sediments were probably deposited by the Kings River. Many irrigation wells in this area are screened in this interval because of the high transmissivity of these sediments. Near drilling site B1, the textures are notably more fine grained at this depth. The sediments near drilling site B1 may be poorly sorted overbank deposits or eroded floodplain muds located adjacent to the main river channel deposits seen in the other boreholes.

Fine-grained floodplain deposits lie directly above the coarse channel deposits, alternating with relatively continuous sequences of coarse sand. Although the fine-grained layers appear to be continuous between borings, there is some uncertainty in this conclusion. The following section on surface geophysical methods will help define the continuity of these layers between borings and out of the two-dimensional vertical plane represented by the wells.

Seismic Reflection

Reflections have been identified in records for a series of single shots along each line to ensure that interpreted events in the processed sections correspond to real reflection information rather than stacked, coherent noise (fig. 5). Reflections are evident at about 90 ms at the 30-m offset and about 155 and 170 ms at larger source-to-receiver distances. Other reflection data are contained within the refracted wave arrival at about 85 to 110 ms. The refracted wave was removed during processing using a tapered mute and a frequency filter.

Reflections were mapped along nearly continuous, vertical profiles from depths of about 34 to 107 m below land surface. The average velocity in this interval is about 1,000 m/s. The calculated vertical resolution is about 3.5 m and the calculated horizontal resolution ranges from 14 to 20 m for reflector depths of 34 to 70 m, based on spectral analysis of the data. Three coherent reflections appear consistent in each of the five profiles at two-way traveltimes of about 70, 100, and 140 ms; a representative section from line 1(fig. 4) is shown in figure 6. The reflections at 70 and 100 ms coincide with sharp contrasts in resistivity and texture as noted in the logs for drilling site B3 (fig. 3) at depths of about 34 and 60 m, respectively. The seismic data confirm that the shallowest reflection at 70 ms is relatively flat, likely corresponding to the transition from fine sand, silt and clay to overlying coarse sands and gravel at drilling sites B2 through B5, at depths ranging from 30 to 34 m. The reflection at about 100 ms correlates with a sharp transition between a scoured silt and clay layer and overlying coarse-grained channel deposits at a depth of about 60 m. The reflection at about 140 ms is located at a depth of about 75 m. A corresponding feature has not been correlated with drilling site B3, suggesting that this interface may not be continuous 152 m south of the seismic profile (where B3 is located); the seismic wave may have responded to a change in physical properties that has not been identified using borehole resistivity measurements, or the interface may be located below the depth of the resistivity log. The interpreted depth of 75 m is very close to the bottom of the borehole. Considering that the vertical resolution of the seismic survey is about 3.5 m, the actual depth may be greater than 80 m at this location. A contrast in resistivity occurs at drilling site B1 at about 78 m (fig. 3), but it is difficult to determine whether this feature should be correlated to the reflection at 140 ms because drilling site B1 is not located near the seismic survey and the resistivity logs are somewhat different at the two sites. Generally, all three reflection events are continuous throughout the surveyed area. The appearance of the deepest reflection as less continuous may be caused by variation in velocity and energy penetration. Deeper reflections are present below 140 ms; however, these events are below the depth of investigation for this study.

The observed "branching" of distinct coherent events, such as at 140 ms at CDP 2,160 (fig. 6), may be caused by increasing layer thickness. In this study, reflections appear to correspond to contacts between coarse, sandy materials, and underlying silt and clay layers where there is sufficient contrast in seismic velocity and density. The bottom of these fine-grained layers has generally not been determined because the layers are probably thinner than the vertical resolution of the data, or the lower transition boundary is more gradational. Several similar features have been identified throughout the records. Most of these features are oriented in one direction: one apparent reflection that branches into two separate events with increasing distance along the line. This might be expected because more points are sampled from features that increase, rather than decrease, in elevation along the survey line; the increase in the number of points is attributed to the ray-path geometry between the source and corresponding receivers.

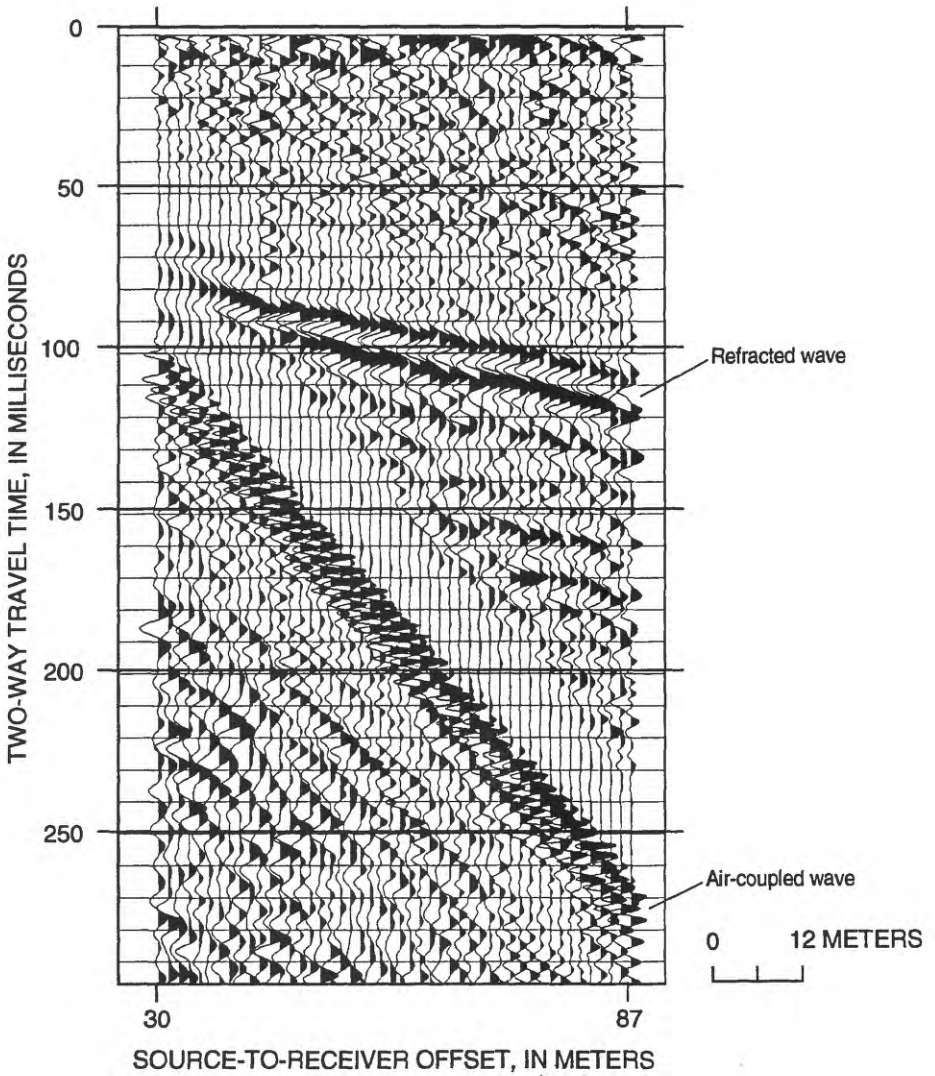

Figure 5. Filtered, scaled shot gather from seismic survey line 1 (see fig. 4). Reflections are apparent at 155 and 170 milliseconds at source-to-receiver offsets from 55 to 87 meters.

Ground-Penetrating Radar

A reflection that appears on nearly all the GPR profiles at about 125 ns, two-way traveltime, is represented in figure 7. This feature may correlate with a 1.5-m thick silt and clay layer at a depth of about 8 m at drilling site B3 (fig. 3), assuming an average EM wave velocity of 0.13 m/ns. This silt and clay layer is very continuous and flat throughout the GPR records, suggesting that it was deposited in the floodplain. At several drilling sites, two fine-grained layers have been distinguished in the borehole (fig. 3) that are not discernible as distinct units on the GPR records. The two silt and clay layers are separated only by a few meters and probably cannot be resolved within the vertical resolution limits of the data. The reflection at 125 ns has variable frequency and amplitude throughout the survey, perhaps because of variations in moisture content or near-surface soils. Because this low-permeability silt and clay layer is only about 8 m below the surface, local variability in irrigation management could have a direct effect on the amount of moisture retained within or immediately above this layer. A reflection at about 210 ns may correspond with the water table. Assuming an average velocity of about 0.13 m/ns, this reflector would be located at a depth of about 14 m, which is consistent with the known

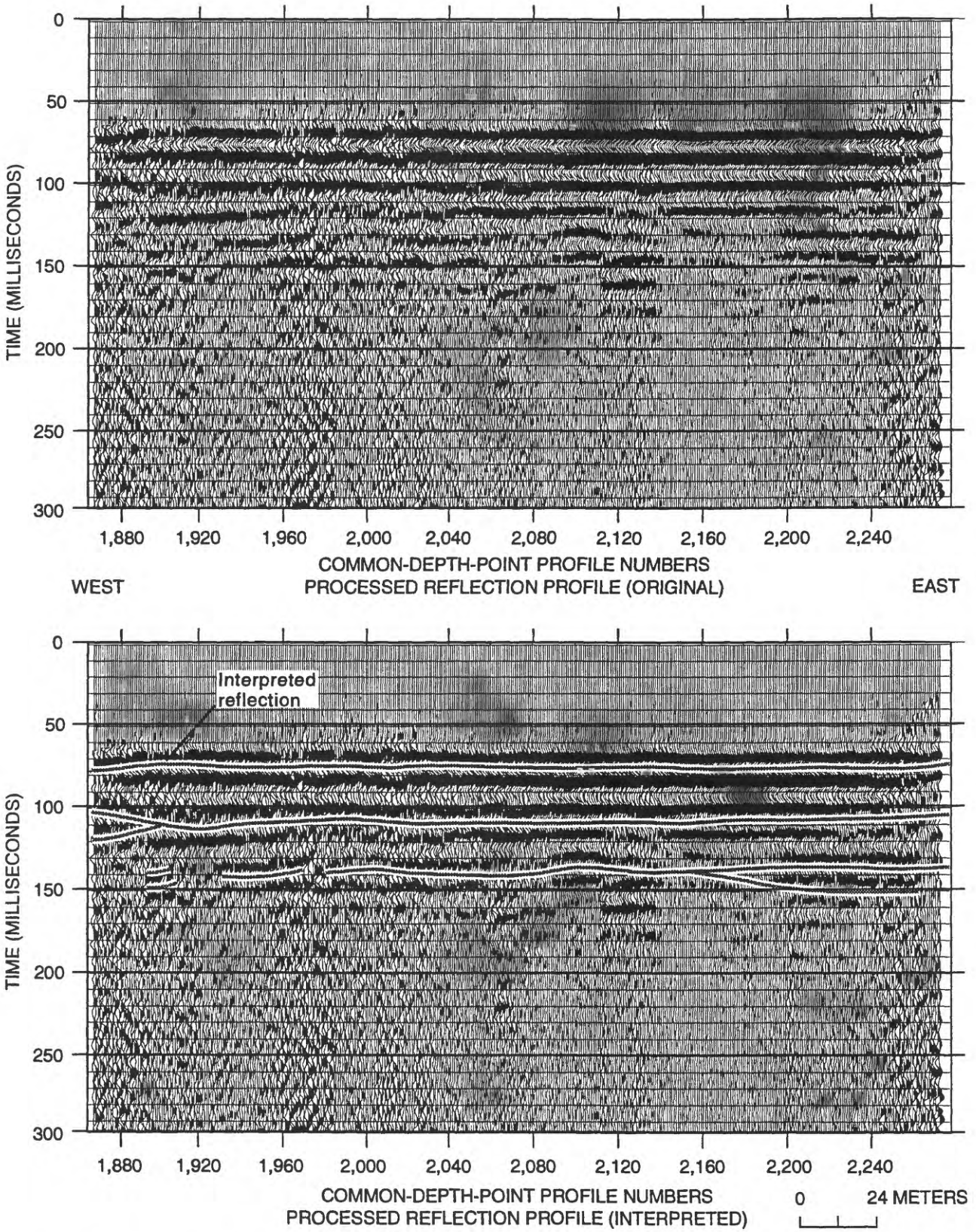

Figure 6. Processed seismic reflection profile from seismic survey line 1, common-depth-point (CDP) station numbers 1,880 to 2,240. Lower section shows interpreted reflections. The reflections at about 70, 100, and 140 milliseconds are interpreted fine-grained layers located at depths of 34, 60, and 75 meters.

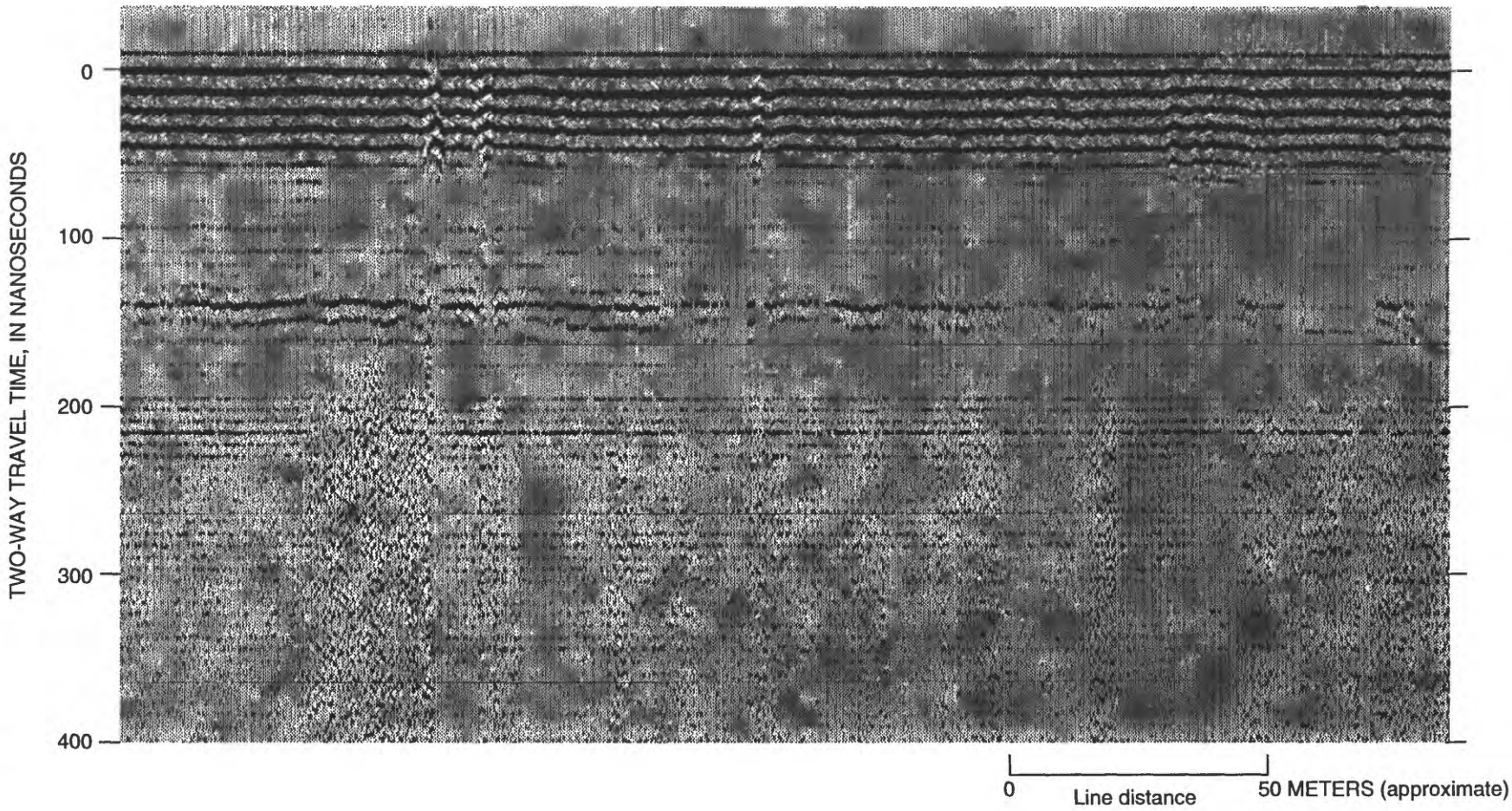

Figure 7. Filtered, scaled ground-penetrating radar (GPR) profile from GPR survey line 2 (see fig. 4). Reflection at about 125 nanoseconds is interpreted as a fine-grained layer located at a depth of 8 meters.

depth-to-water at this study site. At drilling site B3, a silt and clay layer lies immediately above the water table and, therefore, its location may not be separable from a reflection at the water table.

CHARACTERIZATION SUMMARY AND CONCLUSIONS

Descriptions of texture and lithology from 150 m of continuous core provided a basic definition of textural categories for the study site. Sediment textures were categorized into four distinct units based primarily on grain size and degree of sorting. The four textural categories that were present are gravel, coarse sand or gravel, fine sand, and silt and clay, ranked in decreasing order of hydraulic transmissive properties. These sediments, interpreted as distinct hydrogeologic facies, are typical of the fluvial-dominated alluvial fan setting in which they were deposited.

Borehole geophysics was used as a cost-effective, quantitative method to extrapolate the textural categories beyond the extent of the core. In-situ measurements of resistivity were collected in seven borings, providing information on thickness and the vertical sequence of textural categories over a larger area. Although the geophysical logs were not highly correlated with the core, interpretation of the sequence of deposits at each drilling site suggests that the two-dimensional vertical plane represented by the well transect is not aligned exactly with the individual depositional features. The geophysical logs indicate that the sediments below about 60 m are more fine grained.

The interpreted hydrogeologic facies units were extrapolated near sites B2 and B3 using surface geophysical surveys. Together, seismic reflection and GPR methods provided information on depth and lateral extent of four distinct fine-grained facies units ranging in depth from about 8 to 107 m, over a distance of about 3.6 km. Three distinct fine-grained layers were mapped on the seismic profiles along five vertical cross sections at depths of about 34, 60, and 75 m. Average seismic velocity is about 1,000 m/s, and vertical resolution is about 3.5 m. The horizontal resolution ranges from 14 to 20 m at depths of 34 to 70 m. The fine-grained layers were generally continuous in all the seismic profiles. The GPR data were collected along five continuous profiles that coincide with the seismic survey lines. The GPR mapped a relatively continuous fine-grained layer located at a depth of about 8 m, which was interpreted as floodplain-deposited sediments.

Each method discussed in this paper contributes unique information to the characterization of the hydrogeologic facies distribution. The continuous core was important in the determination of the basic textural categories; however, the coring procedure is expensive and time-consuming, so borehole geophysical methods were a rapid, cost-effective alternative to extend the characterization of facies categories beyond the range of the core. The combined borehole methods provided data, such as vertical sequence and thickness of individual facies units. The surface geophysical methods were important in establishing continuity of fine-grained facies, and assisted in the determination of lateral extent of these facies.

The conceptual information provided by this data has been important in understanding the hydrogeologic setting, whereas the quantitative data on vertical sequence, continuity, and lateral extent of the hydrogeologic facies units will be used in the development of a stochastic model of facies distributions in the next phase of this study.

ACKNOWLEDGMENTS

Many individuals provided invaluable assistance and insight during the design and completion of this study and in the publication of the results. In particular, we would like to express our sincere appreciation to the landowners who allowed us access to their property during this investigation. The author would also like to thank Choon Byong Park, Jianghai Xia, Matt Brookshier, and Jack Zedicker for their help in acquiring the seismic reflection data, and David Van Brocklin for his help during acquisition of the ground-penetrating radar data. This study was a cooperative effort of the University of California at Davis and the U.S. Geological Survey.

REFERENCES

Barr, G.L, 1993, Application of ground-penetrating radar methods in determining hydrogeologic conditions in a karst area, west-central Florida: U.S. Geological Survey Water-Resources Investigations Report 92-4141, 26 p.

Beres, M.Jr., and Haeni, F.P., 1991, Application of ground-penetrating-radar methods in hydrogeologic studies: Ground Water, v. 29, no. 3, p. 375-386.

Birkelo, B.A., Steeples, D.W., Miller, R.D., and Sophocleous, M., 1987, Seismic reflection study of a shallow aquifer during a pumping test: Ground Water, v. 25, no. 6, p. 703-709.

California Department of Water Resources, 1993, Groundwater elevation map, January, 1993: Sacramento, Calif., California Department of Water Resources.

Cehrs, D., Soenke, S., and Bianchi, W.C., 1980, A geologic approach to artificial recharge site selection in the Fresno-Clovis area, California: U. S. Department of Agriculture, Science and Education Administration, Technical Bulletin 1604, 73 p.

Dobrin, M.B., 1976, Introduction to geophysical prospecting (3rd ed.): New York, McGraw Hill, 630 p.

Genau, R.B., Madsen, J.A., McGeary, S., and Wehmiller, J.F., 1994, Seismic-reflection identification of Susquehanna River paleochannels on the mid-Atlantic coastal plain: Quaternary Research, v. 42, no. 2, p. 166-175.

Haeni, F.P., 1986, Application of continuous seismic reflection methods to hydrologic studies: Ground Water, v. 24, no. 1, p. 23-31.

Hunter, J.A., Pullan, S.E., Burns, R.A., Gagne, R.M., and Good, R.L., 1984, Shallow seismic reflection mapping of the overburden-bedrock interface with the engineering seismograph—Some simple techniques: Geophysics, v. 49, no. 8, p. 1381-1385.

Keys, W.S., 1990, Borehole geophysics applied to groundwater investigations: U.S. Geological Survey Techniques of Water-Resources Investigations, book 2, chap. E2, 150 p.

Knoll, M.D., Haeni, F.P., and Knight, R.J., 1991, Characterization of a sand and gravel aquifer using ground-penetrating radar, Cape Cod, Massachusetts, *in* Mallard, G.E., and Aronson, D.E., eds., U.S. Geological Survey Toxic Substances Hydrology Program, Proceedings of the Technical Meeting, Monterey, California, March 11-15, 1991: U.S. Geological Survey Water-Resources Investigations Report 91-4034, p. 29-35.

Lieblich, D.A., Haeni, F.P., and Cromwell, R.E., 1992, Integrated use of surface-geophysical methods to indicate subsurface fractures at Tibbetts Road, Barrington, New Hampshire: U.S. Geological Survey Water-Resources Investigations Report 92-4012, 33 p.

Miller, R.D., Steeples, D.W., and Brannan, M., 1989, Mapping a bedrock surface under dry alluvium with shallow seismic reflections: Geophysics, v. 54, no. 12, p. 1528-1534.

Page, R.W., and LeBlanc, R.A., 1969, Geology, hydrology, and water quality in the Fresno area, California: U.S. Geological Survey Open-File Report, 70 p.

Pullan, S.E., and Hunter, J.A., 1991, Delineation of buried bedrock valleys using the optimum offset shallow seismic reflection technique, *in* Ward, S.H., ed., v. 3 of Geotechnical and environmental geophysics: Tulsa, Oklahoma, Society of Exploration Geophysicists, Investigations in Geophysics series, v. 5, no. 3, p. 75-87.

Telford, W.M., Geldart, L.P., and Sheriff, R.E., 1990, Applied geophysics: Cambridge, United Kingdom, Cambridge University Press, 770 p.

Williams, J.H., 1994, Application of electromagnetic-induction logging to ground-water quality studies, *in* Paillet, F.L., and Williams, J.H., eds., Proceedings of the U.S. Geological Survey Workshop on the Application of Borehole Geophysics to Ground-Water Investigations, Albany, New York, June 2-4, 1992: U.S. Geological Survey Water-Resources Investigations Report 94-4103, p. 9-16.

Wright, D.L., Olhoeft, G.R., and Watts, R.D., 1984, Ground-penetrating radar studies on Cape Cod, *in* Neilsen, D.M., and Curl, M., eds., Surface and Borehole Geophysical Methods in Ground Water Investigations: Worthington, Ohio, National Water Well Association, p. 666-680.